Passive photonic elements based on dielectric-loaded surface plasmon polariton waveguides

A. V. Krasavin[a)] and A. V. Zayats
Centre for Nanostructured Media, IRCEP, The Queen's University of Belfast, Belfast BT7 1NN, United Kingdom

(Received 12 April 2007; accepted 25 April 2007; published online 21 May 2007)

The authors present full three-dimensional numerical modeling of passive photonic elements based on dielectric-loaded surface plasmon polariton waveguides (DLSPPWs). They demonstrate that at telecom wavelengths a highly confined SPP mode can be guided in a single mode DLSPPW of subwavelength cross section and estimate the achievable density of photonic integration. The size of bending and splitting photonic elements based on DLSPPW can be as small as a few micrometers with pure bend loss less than 10% (0.4 dB) and the transmission efficiency exceeding 70% (total loss of about 1.3 dB). Such DLSPPW elements are important for implementation of photonic integrated circuits, guiding optical and electric signals in the same circuitry, and lab-on-a-chip applications. © *2007 American Institute of Physics*. [DOI: 10.1063/1.2740485]

Surface plasmon polariton (SPP) waves are becoming widely accepted as a prospective type of optical information carrier in highly integrated photonic devices. SPPs are electromagnetic excitation coupled to electron oscillations propagating in a wavelike fashion along a metal-dielectric interface.[1,2] Optical signals in the form of SPP waves can be efficiently guided and manipulated in waveguiding circuitry having subwavelength dimensions. There exist several approaches to implement plasmonic waveguiding structures based on line defects in surface polaritonic crystals,[3] metallic stripes and wires,[4,5] grooves (gaps) in a metal film,[6,7] a chain of metallic nanoparticles,[8] and metal heterostructures.[9]

Wide metal stripes can be effective SPP waveguides, however, when the width of the stripe becomes small, the losses significantly increase due to scattering on the stripe edges, preventing scaling such waveguides down. In order to overcome this problem, dielectric waveguides for SPPs on a metal surface have been recently proposed[10–12] [Fig. 1(a)]. The dielectric results in a higher refractive index for a SPP wave on a metal-dielectric interface compared to metal-air interface, giving rise to SPP modes bound by the dielectric stripe similar to the guided light modes in conventional optical fibers or planar dielectric waveguides. Thus, stronger confinement and reduction of edge-scattering losses in dielectric-loaded SPP waveguides (DLSPPWs) can be achieved compared to bare metallic stripe waveguides of the same width. Moreover, a dielectric coating can be functionalized to provide thermo-, electro-, or all-optical functionalities and can be used for the development of active plasmonic components. The waveguide can be produced in a very straightforward way by, for example, a direct laser writing on a spin-coated polymer followed by wet etching[10] or by standard means of photolithography [Fig. 1(b)].

Here, using full three-dimensional (3D) finite element numerical simulations, we studied guiding properties of dielectric-loaded SPP waveguides and estimated an achievable level of photonic integration density based on DLSPPW circuitry. We also demonstrated an efficient manipulation of SPP signals in a variety of passive DLSPPW components, such as bends, couplers, and splitters of different designs.

We modeled a dielectric (e.g., polymer with $n_1=1.535$) stripe DLSPP waveguide deposited onto a gold surface ($n_2=0.55+11.5i$, taken from Ref. 13), as depicted in Fig. 1(a). All the numerical simulations are performed at telecom wavelength $\lambda=1550$ nm. At this wavelength a simulated DLSPP waveguide with cross section of 600×600 nm^2 is single mode, supporting a fundamental TM$_{00}$ SPP mode.[12]

As a first step, using two-dimensional (2D) simulations, a spatial distribution of the field of the guided mode has been calculated using an eigenmode solver at the front edge boundary. It reveals a highly localized mode near the dielectric core of the waveguide [Fig. 1(a)]. From the value of the wave vector component along the waveguide, propagation characteristics of the mode can be estimated: effective refractive index $n_{\text{eff}}=1.29$, and propagation length (at which energy of SPP decays in e times due to the Ohmic losses) $L_{\text{prop}}^{2D}\approx43$ μm. These results are consistent with the effective index modeling of such single mode DLSPP waveguides.[12]

In order to perform a full 3D numerical simulation, the field distribution from the 2D simulations was set as a initial boundary condition for 3D analysis. The results confirm the guiding properties of a single mode DLSPPW with no observable radiative losses. The SPP mode propagates along the waveguide, keeping its transverse field distribution constant and its energy exponentially decays with propagation distance due to the Ohmic losses in metal [Fig. 1(c)]. By plotting the dependence of the power flow in the core of the waveguide [Fig. 1(d)], the propagation distance of the SPP mode can be found $L_{\text{prop}}^{3D}=41.3\pm1$ μm, which is consistent with the value predicted in the 2D simulations.

Having proven the validity of the results for 3D SPP mode propagation, we proceeded with modeling of SPP waveguide elements requiring full 3D simulations. First, we investigated coupling between two parallel waveguides in order to determine the cross-talk and achievable density of integration of DLSPPW components. The SPP mode was initially launched in one of the waveguides [right in Fig. 2(a)], and the evolution of the mode was observed during the propagation. It is found that the energy can tunnel into the second waveguide due to the overlap of the waveguide

a)Electronic mail: a.krasavin@qub.ac.uk

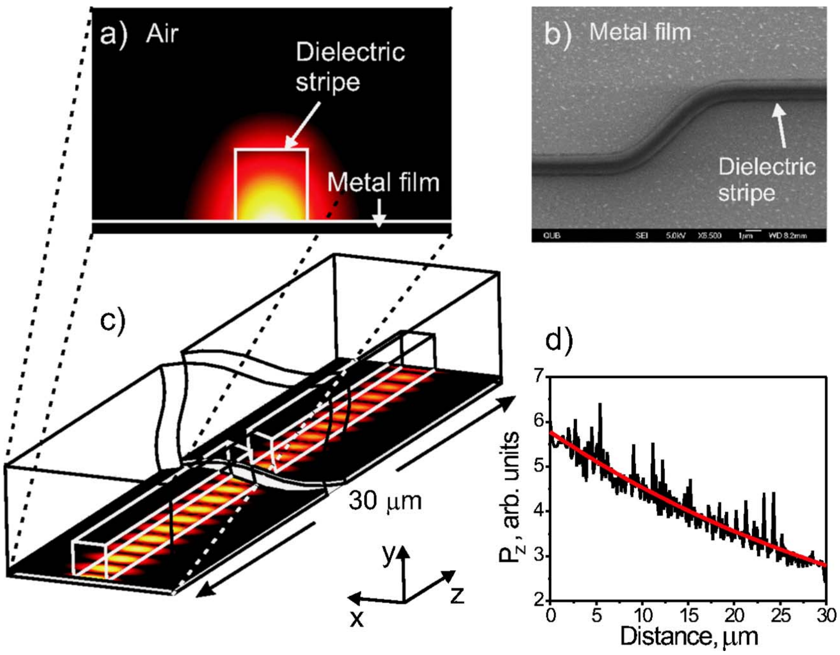

FIG. 1. (Color online) (a) Cross section of 600×600 nm^2 DLSPP waveguide and abs(E_y) field profile of a fundamental TM_{00} SPP mode in it. (b) Scanning electron microscopy image of the DLSPP waveguide fabricated by a direct laser writing on spin-coated polymer layer, as described in Ref. 10. (c) Simulation setup and abs(E_y) field distribution in a straight DLSPP waveguide. (d) Power flow along the center of the waveguide at a distance of 10 nm from the metal surface, the red line is the exponent fit.

modes in the neighboring waveguides. The energy in the second waveguide depends on the distance along the waveguide in harmonic fashion modulated by an exponent, representing the absorption due to the Ohmic losses. The dependence of the coupling distance L_c at which all the energy of the mode is transferred to the neighboring waveguide on the distance between the waveguides cores d is presented in Fig. 2(b). The increase of the coupling length with the distance between the waveguides is exponential. When the waveguides are close to each other, d=700 nm (distance between the waveguide edges of 100 nm), the tunneling between the waveguides is very efficient with L_c=4.6 μm. (This property can be used for designing waveguide couplers and splitters.) When the cores of the waveguides are separated by d=2.6 μm then the coupling between the waveguides is extremely weak ($L_c \sim 2.3$ mm), so at this distance the waveguides are practically not coupled. This gives us a possibility of a high level of integration of the waveguides on a photonic chip.

The first elemental structure required for DLSPP waveguide circuitry is a 90° waveguide bend. We constructed a bend using a waveguide section of a circular shape with a radius R of several micrometers (see the insets of Fig. 3). As observed in the calculated near-field distributions, due to the curvature of the waveguide in the bend, the SPP guided mode is experiencing radiative losses in the form of the SPPs on the surface outside the guide and a free space light when propagating along the curved section. The transmission through the bend $T = I_1/I_0$ was obtained as a ratio between the power flow integrals in the core of the waveguide at the beginning I_0 and at the end I_1 of the bend section. The dependence of the transmission T on a bend radius (Fig. 3, solid line) is determined by a tradeoff between two factors: at small bend radii ("sharp bends"), high radiative losses limit the transmission value as the guided mode energy escapes from DLSPPW; with the increase of the radii, the total length of the bending element increases, leading to higher Ohmic losses during SPP propagation along it. Thus, there is an optimal radius $R \sim 5$ μm, when the total losses of the bend is small, leading to transmission of about 74% (total loss of about 1.3 dB). Moreover, the transmission can be well above 90% corresponding to the bend loss of 0.4 dB (Fig. 3, dashed line) if we make the propagation lossless, for example, by using a gain medium as a dielectric load. The level of possible integration is also fascinating comparing with the planar dielectric waveguides approach, where the size of bending elements is in the millimeter range.[14]

Another key element of integrated optics is a waveguide splitter. We simulated the DLSPP splitter having the most straightforward "fork" form. The distance between the output arms was set to be D=2.6 μm to ensure their optical isolation from each other based on the considerations above. We studied three different shapes of the bend sections of the splitter. Following Ref. 14, where the optimal shapes for S bends of the planar dielectric optical waveguides were discussed, we used the shape of curved sections given by (i) $D/4(1-\cos(\pi z/L_s))$ and (ii) $D/(2L_s)z - D/(4\pi)\sin(2\pi z/L_s)$ and varied the splitter element length L_s. The bend sections were also constructed of the two connected circular arcs with

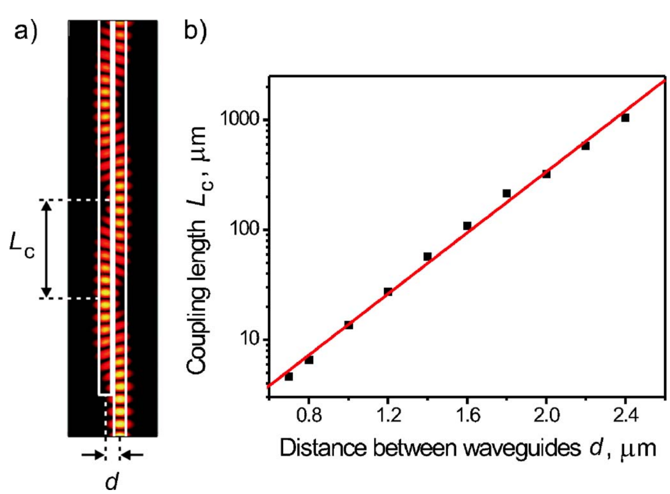

FIG. 2. (Color online) (a) Coupling between two parallel DLSPP waveguides. (b) Dependence of the coupling length L_c on the distance between the waveguide axes d.

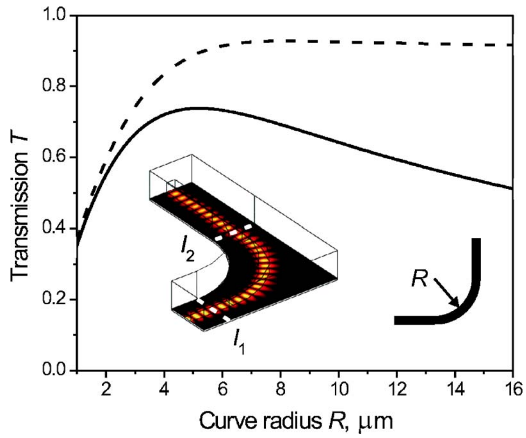

FIG. 3. (Color online) Dependence of the transmission T through a 90° circular bend of the waveguide on the bend radius R, for the waveguides with (solid line) and without (dashed line) Ohmic losses. The inset shows the simulation setup.

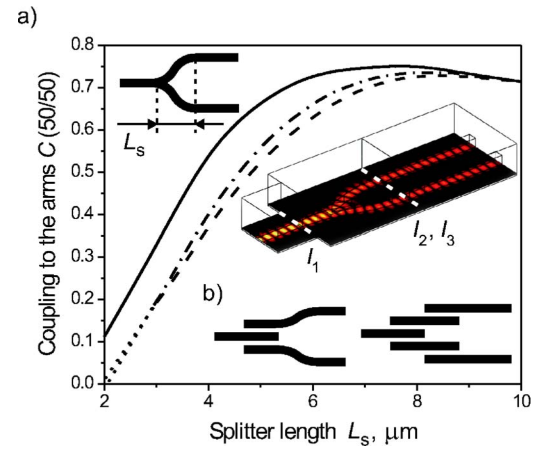

FIG. 4. (Color online) (a) Dependence of the efficiency C of the fork splitter on the length of the splitting element L_s for three shapes described in the text: (solid line) shape (i), (dash line) shape (ii), and (dash-dot line) shape (iii). The inset shows the simulation setup. (b) Other designs of the splitter geometry which have been simulated.

opposite curvature (iii). The angle span of the curvatures was set to obtain a desirable splitter element length and a smooth connection between them. In all three cases the bigger the length of the splitting element, the more smooth is the connection between the input and the output arms, the lower radiative bend losses. However, longer element size leads to the simultaneous increase of the propagation Ohmic losses. (For a splitter, there exists a minimum length of the bend section to satisfy a constraint on optical isolation of the output arms.) The efficiency of coupling to the output arms of the splitter was calculated as $C=(I_1+I_2)/I_0$, where I_0, I_1, and I_2 are the core intensity integrals at the beginning and at the end of the splitter output arms. Due to the symmetry of the splitter, the input mode energy is divided into two equal parts $I_1=I_2$. The dependences of the splitter efficiency on its length for all three shapes are presented in Fig. 4(a). With the increase of the splitter length up to 8 μm the efficiency C monotonously increases, reaching a broad maximum with $C\sim 75\%$ then starts to slowly decrease due to the Ohmic losses. We can see that harmonic shape of the splitter element provides slightly better efficiency in comparison with the other two, showing similar results. Again, the coupling efficiency of the splitter can be more than 90% for the lossless waveguiding.

We also considered other designs of the splitter, particularly based on the tunnel-coupling mechanism between two parallel waveguides, as discussed above [see Fig. 4(b)], in each case performing the optimization of the geometry. However, such designs provide similar level of the splitting efficiency as observed above.

In conclusion, using 3D numerical simulations we have characterized and optimized the main passive photonic elements based on dielectric-loaded SPP waveguide technology. The results show that a very high photonic integration density can be achieved with a distance between the waveguides just ~ 2.5 μm at the telecom wavelength range. We demonstrated an efficient ($>70\%$) DLSPP waveguide bending and splitting elements of just a few micrometer size. Moreover their efficiency can be more than 90% if the propagation (Ohmic) losses are compensated. Such DLSPPW photonic elements are extremely beneficial in comparison with conventional planar waveguide technology (which can provide similar loss parameters only in millimeter length scale of bend elements) and can find applications in photonic and optoelectronic integrated circuits and lab-on-a-chip sensing.

This work was supported in part by EPSRC (UK) and EC FP6 STREP PLASMOCOM. The authors acknowledge the fruitful discussions with G. A. Wurtz, S. I. Bozhevolnyi, and P. Bayvel.

[1]H. Raether, *Surface Plasmons on Smooth and Rough Surfaces and Gratings* (Springer, 1988).
[2]A. Zayats, I. Smolyaninov, and A. Maradudin, Phys. Rep. **408**, 131 (2005).
[3]V. Volkov, S. Bozhevolnyi, K. Leosson, and A. Boltasseva, J. Microsc. **210**, 324 (2003).
[4]J. Krenn and J.-C. Weeber, Philos. Trans. R. Soc. London **362**, 739 (2004).
[5]J. Takahara, S. Yamagishi, H. Taki, A. Morioto, and T. Kabayashi, Opt. Lett. **22**, 475 (1997).
[6]S. Bozhevolnyi, V. Volkov, E. Devaux, J.-Y. Laluet, and T. Ebbesen, Nature (London) **440**, 508 (2006).
[7]L. Chen, B. Wang, and G. P. Wang, Appl. Phys. Lett. **89**, 243120 (2006).
[8]S. Maier and H. Atwater, J. Appl. Phys. **98**, 1 (2005).
[9]B. Wang and G. Wang, Appl. Phys. Lett. **90**, 013114 (2007).
[10]C. Reinhardt, S. Passinger, B. Chichkov, C. Marquart, I. Radko, and S. Bozhevolnyi, Opt. Lett. **31**, 1307 (2006).
[11]B. Steinberger, A. Hohenau, H. Ditlbacher, A. L. Stepanov, A. Drezet, F. Aussenegg, A. Leitner, and J. Krenn, Appl. Phys. Lett. **88**, 094104 (2006).
[12]T. Holmgaard and S. Bozhevolnyi *et al.*, Phys. Rev. B (to be published).
[13]*Handbook of Optical Constants of Solids*, edited by E. D. Palik (Academic, New York, 1984), 294.
[14]A. Kumar and S. Aditya, Microwave Opt. Technol. Lett. **19**, 289 (1998).